The Journal of Experimental Biology 212, 2564-2570
Published by The Company of Biologists 2009
doi:10.1242/jeb.032532

# Reduction in fragile X related 1 protein causes cardiomyopathy and muscular dystrophy in zebrafish

Sandra van't Padje[1,*], Bill Chaudhry[2,*], Lies-Anne Severijnen[1], Herma C. van der Linde[1], Edwin J. Mientjes[1], Ben A. Oostra[1] and Rob Willemsen[1,†]

[1]CBG-Department of Clinical Genetics, Erasmus MC, 3015 CE Rotterdam, The Netherlands and [2]Institute of Human Genetics, Newcastle University, Newcastle upon Tyne NE1 3BZ, UK

*These authors contributed equally to this work
†Author for correspondence (e-mail: r.willemsen@erasmusmc.nl)

Accepted 19 May 2009

## SUMMARY

**Lack of the *FMR1* gene product causes fragile X syndrome, the commonest inherited cause of mental impairment. We know little of the roles that *fragile X related* (*FXR*) gene family members (*FMR1*, *FXR2* and *FXR1*) play during embryonic development. Although all are expressed in the brain and testis, *FXR1* is the principal member found in striated and cardiac muscle. The *Fxr1* knockout mice display a striated muscle phenotype but it is not known why they die shortly after birth; however, a cardiac cause is possible. The zebrafish is an ideal model to investigate the role of *fxr1* during development of the heart. We have carried out morpholino knockdown of *fxr1* and have demonstrated abnormalities of striated muscle development and abnormal development of the zebrafish heart, including failure of looping and snapping of the atrium from its venous pole. In addition, we have measured cardiac function using high-speed video microscopy and demonstrated a significant reduction in cardiac function. This cardiac phenotype has not been previously described and suggests that *fxr1* is essential for normal cardiac form and function.**

Supplementary material available online at http://jeb.biologists.org/cgi/content/full/212/16/2564/DC1

Key words: *fxr1*, morpholino, knockdown, cardiomyopathy, muscular dystrophy.

## INTRODUCTION

*FMR1* and the structurally related *FXR1* and *FXR2* genes produce the fragile X related (FXR) family of proteins (FMRP, FXR1P and FXR2P, respectively), which have RNA-binding capability *via* two KH domains and one RGG box (Ashley et al., 1993; Siomi et al., 1993). FXR proteins are found to be associated with ribosomes in the form of messenger ribonuclear particles (mRNP) (Feng et al., 1997; Tamanini et al., 1996) and it is thought they mediate transport of specific mRNAs to different intracellular compartments and inhibit translation of their target mRNAs. Interestingly, whereas all three genes are highly expressed in the brain and testis, only FXR1P is strongly expressed in skeletal muscle tissue where it localises to the Z-lines and costameres (Bakker et al., 2000; Dube et al., 2000; Mientjes et al., 2004). In striated muscle tissue, two different FXR1P isoforms of 82 kDa and 84 kDa size are found due to transcriptional splicing activity but the functional relevance of these isoforms is unknown (Dube et al., 2000). Recently, a high affinity for mRNAs containing a G-quartet has been demonstrated for the longest FXR1P isoform that is highly expressed during myogenesis and in adult cardiac and skeletal muscle tissue (Bechara et al., 2007).

Whilst FMRP has been extensively studied due to its involvement in the fragile X syndrome, no human disease relating to the dysfunction of *FXR1* and *FXR2* have been described so far. Mouse mutants null for *Fmr1*, *Fxr1* and *Fxr2* have been generated (Bakker et al., 1994; Bontekoe et al., 2002; Mientjes et al., 2004). *Fxr1* knockout mice died shortly after birth and, in keeping with the high expression levels of the gene in skeletal muscle, these *Fxr1* null mice demonstrate disruption of the cellular architecture of skeletal (striated) and cardiac muscle tissue (Mientjes et al., 2004). The cause of death is not clear but the absence of Fxr1p, with consequent delocalisation of dystrophin and alpha-actinin from the costameres (Mientjes et al., 2004), appears to be relevant in the skeletal muscle dystrophy and may also be important in cardiac function. The *FXR1* gene shows evolutionary conservation, and morpholino (MO) knockdown in *Xenopus* has suggested abnormal somite formation (Huot et al., 2005). We have previously shown that the functional domains of *FXR* genes are conserved in zebrafish and that the expression pattern of Fxr1 in zebrafish is similar to human and mouse (Engels et al., 2004). Furthermore, the mRNA sequence around the initiator codon of *fxr1* is known and it has therefore proved possible to investigate the effects of translational silencing using morpholino techniques. In the present study we have demonstrated abnormalities of striated muscle development due to knockdown of *fxr1* in the zebrafish. Moreover, we have carried out a structural and functional analysis of cardiac function in the absence of this gene product and have shown a severe embryonic cardiomyopathy, which results in heart failure, a failure of normal heart looping and the snapping of the heart from its venous connections.

## MATERIALS AND METHODS

### Zebrafish strains and care

The zebrafish (*Danio rerio* Hamilton 1822) strains used for this work were the Wageningen ZF WT Zodiac F5 line and the AB line (ZIRC Oregon, OR, USA). Embryos were all raised at 28.5°C, and adult fish were maintained at 26°C on a 14 h:10 h light:dark cycle. Developmental stages were determined according to Kimmel (Kimmel et al., 1995).

### Morpholino injection

Two non-overlapping morpholino antisense oligonucleotides designed for translational blocking of *fxr1* mRNA were obtained from Gene-Tools (Philomath, OR, USA): MO-AUG=5′-GTCAG-TTCCTCCATGTTGAGCGCGA-3′; MO-UTR=5′-GATGCTG-GGTAAAGTTCCAGAAC-3′. Morpholinos were reconstituted in distilled water and further diluted in Danieau solution containing 0.05% Phenol Red (Sigma Chemical Co., St Louis, MO, USA) for injection. Yolk injections were carried out using eggs before the four-cell stage, using a pneumatic picopump (World Precision Instruments, Berlin, Germany). Different amounts of *fxr1* morpholino were injected to determine the optimum dose of *fxr1* morpholinos (1–16 ng). As the observed phenotype was dosage-dependent, most of the analysis experiments were carried out following injection with either 4 or 8 ng of *fxr1* morpholinos. Rescue of the morpholino phenotype was achieved by coinjecting mRNA encoding full-length *Xenopus fxr1* with 8 ng MO-AUG (see Fig. S1 in supplementary material for details).

### Western blot analysis

In order to demonstrate effective knockdown of Fxr1 protein production, western blots were performed using stage-matched embryos and morphants (8 ng) at 24, 48 and 72 h.p.f. (hours postfertilisation) as previously described (van't Padje et al., 2005). Briefly, following blocking of gels, an antibody against zebrafish Fxr1p (Affi5, 1:500) was applied (Engels et al., 2004). Following washing, a peroxidase conjugated secondary antibody (goat anti-rabbit Igs; 1:5000) was used to detect specific antibody binding and reported by chemiluminescence (ECL Kit, Amersham, UK). To demonstrate equivalent loading of lanes, the same gels were stained using AC-40, a pan-actin antibody (Sigma Chemical Co., 1:1000). The gel bands obtained were quantified using TotalLab v2.01 (Biosystematica, Ceredigion, Wales, UK).

### Histology, immunohistochemistry, whole mount *in situ* hybridisation and whole mount immunofluorescent labelling

Histological staining (Haematoxylin and eosin) and immunohistochemistry were performed as previously described using either paraffin (5 μm) or glycomethacrylate (1 μm) sections (van't Padje et al., 2005). The primary antibodies used for immunolabelling were: anti-alpha-actinin (Sigma Chemical Co.), Mandra1 anti-dystrophin (Sigma Chemical Co.) and anti-vinculin (sc-7649, Santa Cruz, CA, USA). Appropriate anti-mouse or anti-goat immunoglobulin peroxidase conjugates (1:100) were used as secondary antibodies and the labelling reported using DAB (Sigma Chemical Co.). Whole mount immunofluorescence labelling of hearts was carried out using S46 and MF20 antibodies (Developmental Studies Hybridoma Bank, University of Iowa, IA, USA) as described (Keegan et al., 2004).

Whole mount *in situ* hybridisation was performed with digoxigenin (DIG)-labelled RNA probes as previously described (Thisse et al., 1993). The *MyoD* and *cardiac myosin light chain 2* (*cmlc2*) riboprobes were kind gifts from the Hubrecht Laboratory, Utrecht, The Netherlands (Weinberg et al., 1996; Yelon et al., 1999).

### Assessment of cardiac function

Movies were taken using a high-speed digital video camera (640×480 pixels at 130 frames $s^{-1}$) (Multipix Imaging, Hampshire, UK). Measurement of cardiac chamber volumes was carried out at end diastole and end systole by the method of Sandler and Dodge, which assumes the chambers to be ellipsoids of revolution (Sandler and Dodge, 1968). Averaged data were expressed as arithmetic means ± s.e.m.; statistical significance was assessed by Student's *t*-test.

## RESULTS

### Developmental expression of *fxr1* and morpholino knockdown of Fxr1

Knockdown of Fxr1 during early zebrafish development was effectively achieved using translation blocking antisense morpholino oligonucleotides. A first morpholino was designed to complement the start site AUG (MO-AUG), and specificity of knockdown was shown using a second morpholino designed to complement the 5′ untranslated region (MO-UTR) of the zebrafish *fxr1* mRNA. The successful reduction in Fxr1 by both morpholinos was demonstrated by western blotting using an antibody specific to zebrafish Fxr1. Both MO-AUG and MO-UTR (8 ng) were injected into the yolk of embryos prior to the four-cell stage and compared with stage-matched wild type (WT) embryos at 24, 48 and 72 h.p.f. Only blot data for MO-AUG are shown as the MO-UTR results were the same (Fig. 1). The blots exhibited both the Fxr1 isoforms, the 73 kDa isoform being more prominent at 24 h but at 48 and 72 h.p.f. levels of the 73 kDa and 75 kDa isoforms were equivalent. Homogenates from MO-AUG and MO-UTR morpholino-injected embryos showed a significant reduction in Fxr1 expression levels until 72 h.p.f. Quantification of the gels, using pan-actin staining as a loading control, suggested that knockdown of Fxr1 protein was to at least 22%, 16% and 12% of WT levels at 24, 48 and 72 h.p.f., respectively.

### Abnormal myotome formation in *fxr1* morphants

The *fxr1* morphant phenotype showed a dosage-dependent effect, which was not seen in rescue experiments carried out by microinjection of a mixture of 8 ng AUG-MO and 4 ng *fxr1* RNA (77% rescue; *N*=80). The severity of the phenotype increased with higher MO doses. Abnormal tail formation was apparent at 24 h.p.f. with more severe tail curling with 8 ng *fxr1* morpholino compared with WT (Fig. 2A–C). The same tail appearances were seen at 48 h.p.f. but some embryos with relatively normal myotome formation were seen to have significant pericardial effusions (compare Fig. 2D with 2E). The typical appearance at 72 h.p.f. ranged from a relatively normal tail (Fig. 2F for WT and Fig. 2G for 4 ng MO-AUG) to a significantly curved tail (Fig. 2H) and, at high

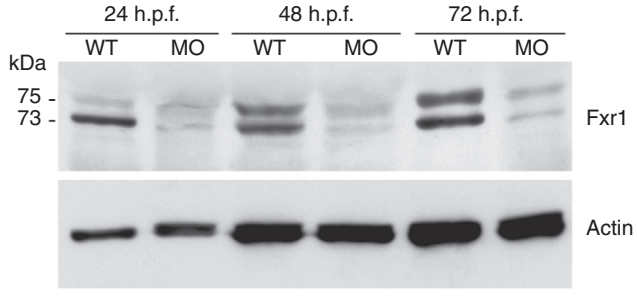


Fig. 1. Western blot analysis of homogenates from embryos injected with 8 ng MO-AUG (MO) and stage-matched wild type (WT) embryos at 24, 48 and 72 h.p.f. (hours postfertilisation). Two isoforms of Fxr1 (73 kDa and 75 kDa) were recognised using Affi5, a rabbit specific antibody generated against zebrafish Fxr1. The 73 kDa isoform of Fxr1 predominated at 24 h.p.f. but at 48 and 72 h.p.f. the levels of the 73 kDa and 75 kDa isoforms were approximately equal. Homogenates from embryos injected with MO-AUG showed a significant reduction in expression of both Fxr1 isoforms. Immunoblotting with pan-actin, AC40 antibody demonstrated equivalent gel loading.

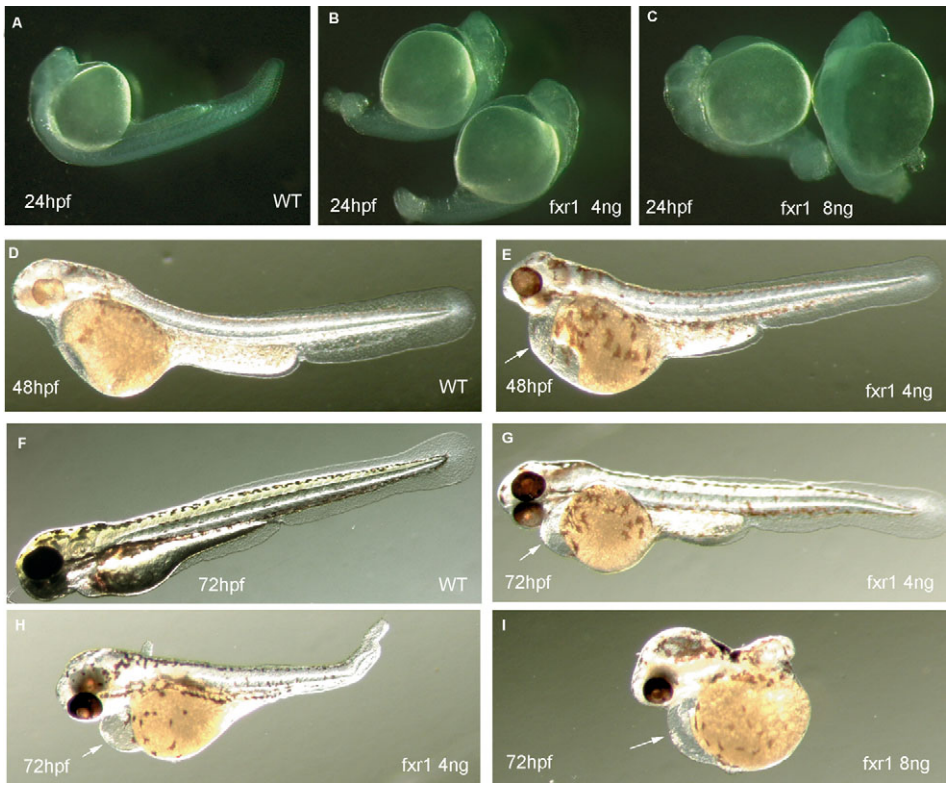


Fig. 2. The *fxr1* morphant phenotype. Translation blocking morpholinos directed against the 5′ UTR region and AUG site produce the same dose-dependent effects: B, E, G and H were injected with 4 ng; C and I were injected with 8 ng of AUG-MO. A, D and F are wild type (WT). There is a dose-dependent disruption to tail formation at 24 h.p.f. (hours postfertilisation) (B and C) with increasing severity of tail curling and shortening. A similar spectrum of mild (G) to moderately severe (H) disturbance of tail formation was observed with 4 ng injections at 72 h.p.f. The severest phenotype, demonstrating complete absence of tail formation, was observed only after 8 ng injections (I). Pericardial oedema (arrows) is seen in embryos injected with 4 ng of morpholino despite mild tail abnormalities (E and G) and in more severely affected embryos (H), including those at higher doses (I).

morpholino doses (8 ng), a shortened or absent tail (Fig. 2I). The milder phenotypes were more apparent (82%; *N*=243) at the lower dose (4 ng) and the more severe phenotypes (79%; *N*=256) at the higher dose (8 ng).

All of the *fxr1* morphants demonstrated 'U'-shaped rather than the normal 'V'-shaped somites and the horizontal myoseptum was absent (Fig. 3A,B). These anatomical features were reflected in poor motility, such that despite vigorous activity on contact stimulation, they were not able to swim far or were only able to spin around one point.

Haemotoxylin and eosin staining of sections from paraffin-embedded 48 h.p.f. morphants revealed disorganisation of striated muscle within the myotomes such that the muscle fibres were loosely arranged and the myotomes were arranged in oblique rather than longitudinal orientations. In low dose morphants (4 ng), myoseptae between the myotomes were still recognisable at the anterior part of the tail; however, in the more posterior areas of the tail no myoseptae were visible and striations within muscle cells could not be seen (Fig. 3C,D). The high dose morphants (8 ng) had more severe disruption of the muscle architecture extending to the most anterior parts of the tail and in the most severely affected the myotomes were absent (data not shown). Embryos were also embedded in glycomethacrylate resin (GMA) and 1 μm semi-thin sections prepared to demonstrate the sarcomeric morphology. In control embryos, and also at the proximal part of the tail of the *fxr1* morphants, the nuclei of the sarcomeres had the expected oval shape (Fig. 3E). However, nuclei of the sarcomeres within the distal part of the tail of *fxr1* morphants remained rounded until 96 h.p.f. (Fig. 3F), indicating a delay in differentiation.

### Abnormal MyoD patterning in *fxr1* morphants

The shortened tail segment and the delayed differentiation of muscle cells suggested a possible disruption of MyoD expression. This master regulator gene of the myogenic gene programme plays a crucial role in the expression of muscle structural proteins and in the assembly of myofibres (Tapscott, 2005). We therefore carried out whole mount *in situ* hybridisation of embryos with antisense probe to MyoD at the 10–11 somite stage. In WT control embryos two longitudinal stripes lateral to the notochord with clearly visible accompanying lateral bands were observed. By contrast, *fxr1* morphants (8 ng dose AUG-MO only) at the 10–11 somite stage showed shorter lateral bands with smaller perpendicular extension (Fig. 3G,H).

### Mis-localisation of dystrophin in striated muscle cells

The cytoskeletal components of the skeletal myocytes were examined by immunohistochemistry performed on paraffin sections using WT and *fxr1* morphants (only 8 ng AUG-MO dose). Alpha-actinin, a costameric cytoskeletal component, was strongly expressed in control embryos, clearly demonstrating large and ordered myocytes inserting into myotendinous junctions (Fig. 4A,C). However, *fxr1* morphants showed disruption to the number of myocytes, which was more evident in the distal parts of the tail rather than the proximal parts (Fig. 4B) and myocytes were randomly arranged and many muscle cells stained less strongly than normal (Fig. 4D). In control embryos, robust dystrophin labelling was seen along the length of the 'V'-shaped myoseptae (Fig. 4E). This was not so in the morphants where portions of the 'U'-shaped myoseptum labelled with dystrophin antibody but other parts did not, despite the presence of a well formed myoseptum in that area (Fig. 4F). Vinculin labelling in control embryos was localised to the 'V'-shaped myoseptae as well as to the surface of the myocytes (Fig. 4G). In morphants this localisation was well preserved, although with the disordered muscle architecture it is not possible to comment whether this is at normal or increased levels (Fig. 4H).

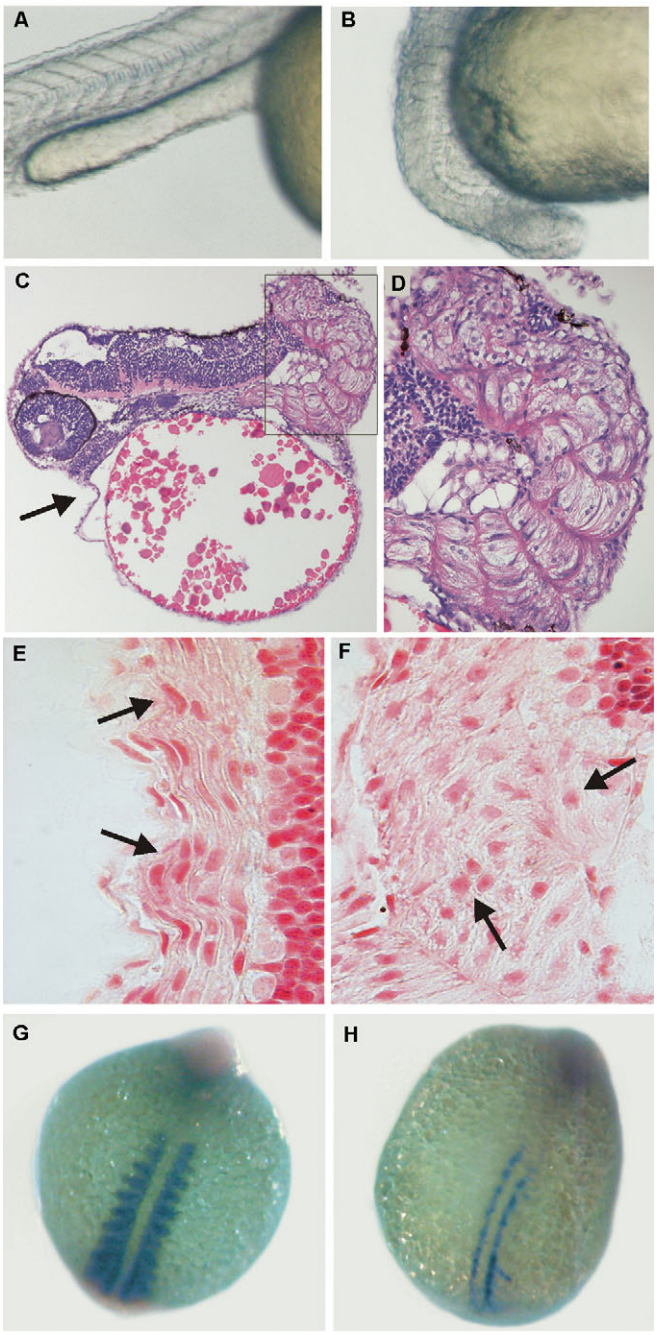


Fig. 3. Disruption of myotome formation using AUG-MO (similar results for UTR-MO). (A) Brightfield image of 24 h.p.f. (hours postfertilisation) control embryo showing well defined 'V'-shaped somites and horizontal myoseptum. (B) Brightfield image of 24 h.p.f. 4 ng morphant showing disruption of normal tail formation with the loss of horizontal myoseptum and 'U'-shaped somites. (C) Longitudinal section of 72 h.p.f. wax-embedded morphant stained with haematoxylin and eosin, showing pericardial oedema (arrow) and moderate disturbance to tail/myotome formation. Closer inspection (D) demonstrates the absence of a horizontal myoseptum and irregular patterning of myofilaments, which are more pronounced in the caudal region. Nuclear morphology indicating delayed myocytes development. High power examination of eosin-stained resin sections (1 μm) of normal skeletal muscle from a 72 h.p.f. control embryo (E) shows elongation of nuclei (arrows). By contrast, nuclei from a 4 ng morphant are spherical (arrows), suggesting a delay in myocyte development (F). Whole mount *in situ* hybridisation with riboprobe for zebrafish *MyoD* mRNA. The characteristic parallel bands of *MyoD* expression either side of the notochord are demonstrated in a wild type (WT) embryo at 14 h.p.f. (G). A pattern of perpendicular stripes superimposed upon these indicates *MyoD* expression within the somites. In the 8 ng *fxr1* morphant, the parallel bands do not extend as far caudally as they do in the WT. The perpendicular somitic expression stripes are faint and do not extend laterally (H).

### Severe mechanical cardiac failure

Fxr1 is strongly expressed in the atrial and ventricular myocytes of control embryos at 48 h.p.f., the earliest stage examined (Fig. 5A). In *fxr1* morphants (AUG-MO only), the initial formation of the midline heart cone was observed to occur normally at approximately 22 h.p.f. and extension of the primary heart tube occurred normally. As with WT embryos, the heart began waves of contraction at this time and there was no evidence of developmental delay in these processes (data not shown). Intrinsic rhythmicity had increased by 28 h.p.f. and forward flow of blood cells through the heart and peripheral circulation was seen in both morphants and control embryos. Atrioventricular cushion tissue, present as an area of cuboid-shaped cells at the junction between the atrium and ventricle, was seen in both normal and morphant embryos at 48 h.p.f. (Fig. 5B,C, arrows). However, at this relatively late stage of zebrafish cardiogenesis the morphant heart remained a relatively tubular structure (Fig. 5C) when compared with the control embryo heart, which had an obvious waist at the level of the atrioventricular junction and more spherical chamber morphology (Fig. 5B). Whole mount *in situ* hybridisation studies, probing for *cmlc2* transcripts at 56 h.p.f., demonstrated that both control and morphant embryos contained abundant mRNA but that the morphant hearts had failed to undergo looping (Fig. 5D,E). In order to determine whether the atrial and ventricular chambers were normally present, whole mount antibody labelling, with MF20 (which recognises both atrial and ventricular cardiomyocytes) and S46 antibody (which recognises atrial myocytes) was undertaken. Whilst these studies demonstrated normal chamber specification, they also served to emphasise the failure of looping. In control embryos the atrium (Fig. 5F) and the ventricle (Fig. 5G) always lay in different focal planes. In morphants however both the atrium and ventricle could be seen to lie in the same focal plane (Fig. 5H–J). In most 4 ng morphants, the proximal tip of the atrial chamber, at its venous inlet, was narrowed to form a thin walled fine tube, which was labelled as atrial tissue (Fig. 5H, arrow). In most 8 ng morphants, this appeared to be stretched to a long thread and this often appeared to have snapped, leaving the beating heart free floating in the pericardial cavity, tethered only by the ventriculo–bulbar connection (Fig. 5I). In other cases, the atrial chamber appeared to become stretched to a long thin tube. The inner lumen of the atrial chamber was usually narrowed to impede the passage of blood cells, although the ventricular chamber did not become stretched and maintained a more rounded morphology. Although in some morphants circulation of blood through the tail may have been disturbed as a consequence of abnormal myotomes, the heart abnormalities were still present even in those morphants with well-preserved caudal structures and patent dorsal aorta and cardinal veins.

The disturbance in cardiac development was also manifest in abnormal cardiac function. In WT embryos, the heart rate normally increases over the first days of life to approximately 120 beats $min^{-1}$ by 72 h.p.f. (Schwerte et al., 2005). This was seen in WT controls and importantly also in our rescued embryos. However, the heart rate at 72 h.p.f. was reduced to 97 beats $min^{-1}$ in 4 ng morphants and to 66 beats $min^{-1}$ in 8 ng morphants (data not shown).

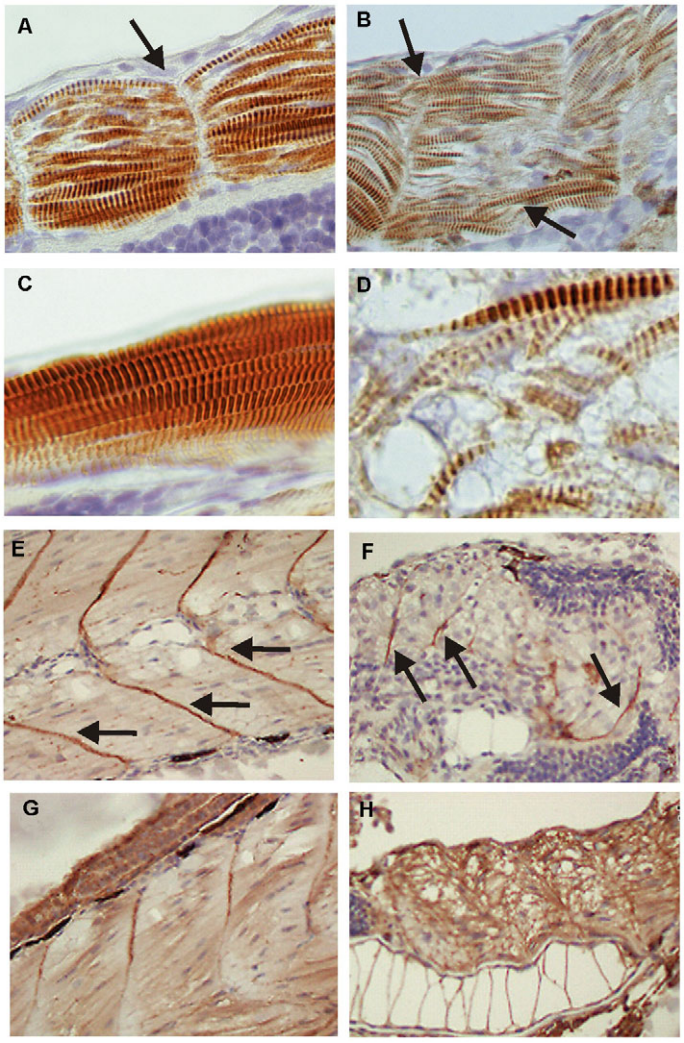


Fig. 4. Immunohistochemical labelling of cytoskeletal proteins in myotomes of 72 h.p.f. (hours postfertilisation) wild type (WT) control (A, C, E and G) and 8 ng morphants (B, D, F and H). Labelling of longitudinal wax sections with anti-alpha-actinin demonstrates ordered and parallel myocytes formed with the myotome and inserting into the myoseptum (arrows) (A). In the morphant the myoseptae are irregularly placed (arrows) and although myocytes are relatively normally arranged at the rostral end (left) there is increasing disorder in the caudal regions. High power examination of the myocytes reveals strong dense staining for alpha-actinin in the control embryos (C) but variable staining of disorganised myocytes in seen in the morphants (D). The myoseptae (arrows) demonstrate strong labelling with dystrophin along their entire length in WT control sections (E) but the labelling of dystrophin occurs only in patches of the myoseptae (arrows) in the morphants (F). By contrast, widespread vinculin labelling was seen throughout the myocytes and at the myoseptae of morphants (H). After making allowances for the disorganised structures the staining pattern is similar to that in control embryos (G).

We assessed heart function in 4 ng *fxr1* morphants at 72 h.p.f. by ejection fraction rather than by instantaneous velocity of red cells in the dorsal aorta to avoid potential distortions of data due to tail malformations. In normal embryos the time of maximal atrium filling occurs when its walls are relaxed and it is pulled distally by maximal ventricular contraction (Fig. 5K). Similarly the maximal phase of ventricular filling is when the ventricular wall is relaxed and the atrium has fully ejected through the atrioventricular valve (Fig. 5L). Thus, atrial end diastole occurs at the same moment as end ventricular systole, and ventricular end diastole occurs at the time as atrial end systole. In control embryos the atrial ejection fraction was 63% (±7% s.e.m.) whereas in the *fxr*1 morphants the atrial ejection fraction was 37% (±11%). In control embryos the ventricular ejection fraction 68% (±8% s.e.m.) and in morphants the mean ventricular ejection fraction was 17% (11% s.e.m.) (Fig. 5O).

## DISCUSSION

In the present study, the specificity of Fxr1 knockdown has been demonstrated by the highly reproducible phenotypes obtained with two different non-overlapping morpholinos specific for this gene and western blotting using an antibody specific for Fxr1. The lack of these findings when injecting a mismatch morpholino control not only supports this specificity but also excludes disruption of myotomes and pericardial oedema as non-specific effects of morpholino studies (Ekker and Larson, 2001). Importantly, we did not see other non-specific features of morpholino use, such as widespread cell death. An additional advantage of this technique over other mutant models is that maternally provided mRNA is also suppressed by the translational blocking morpholinos.

A reduction in MyoD expression during somite formation was first noted in *Xenopus* experiments (Huot et al., 2005). We have confirmed and extended this finding in our current zebrafish studies. It appears that shortening of the MyoD stripe length and the domains of expression within each somite is sufficient to prevent the most caudal myotomes forming or render them severely dyslastic. However, we have no explanation as to why there is more severe disruption to caudal myotomes than proximal ones. In addition to this effect on myotome specification, the presence of 'U'-shaped tail somites in *fxr1* morphants suggests a defect in the formation of the horizontal myoseptum and is characteristic of defects in slow muscle development (Ingham and Kim, 2005). We have also shown that the myocyte organisation within the myotome is abnormal, not only in the organisation of the muscle fibres themselves but also with regard to the compartmental organisation of the myocytes. Skeletal and cardiac muscle cells both have regular points of attachment to the supporting extracellular matrix known as costameres. Connection to the Z-bands occurs at these points through vinculin and other related connecting proteins such as talin among many others (Samarel, 2005). The localisation of these attachments is developmentally as well as functionally important as they are sites of formation of pre-myofibrils in immature myocytes. Interestingly our data suggest that vinculin and alpha-actinin are present at the level of costameric attachments although levels of immunostaining may be reduced. A second form of attachment is provided by dystrophin and the dystrophin associated protein complex (DAPC). These complexes link the actin cytoskeleton to laminin $\alpha 2$ and are enriched at junctional and non-junctional regions of the sarcolemma, such as connections between myocyte and myocyte, myocyte and tendinous tissue, and the neuromuscular junction. In order to examine DAPC we looked at dystrophin expression and noted this to be reduced in the abnormal myoseptal areas. This finding supports a role for Fxr1 in transport and regulation of translation of specific mRNAs to the myotendinous junction, as it is known that dystrophin mRNA is transported to and translated within specific cellular compartments whereas other cytoskeletal proteins, such as vinculin are first found throughout the cytoplasm and then localise to membranes (Samarel, 2005). Originally, it has been hypothesised that Fxr1 acts as a repressor of translation in the RNA-induced silencing complex (RISC); however,

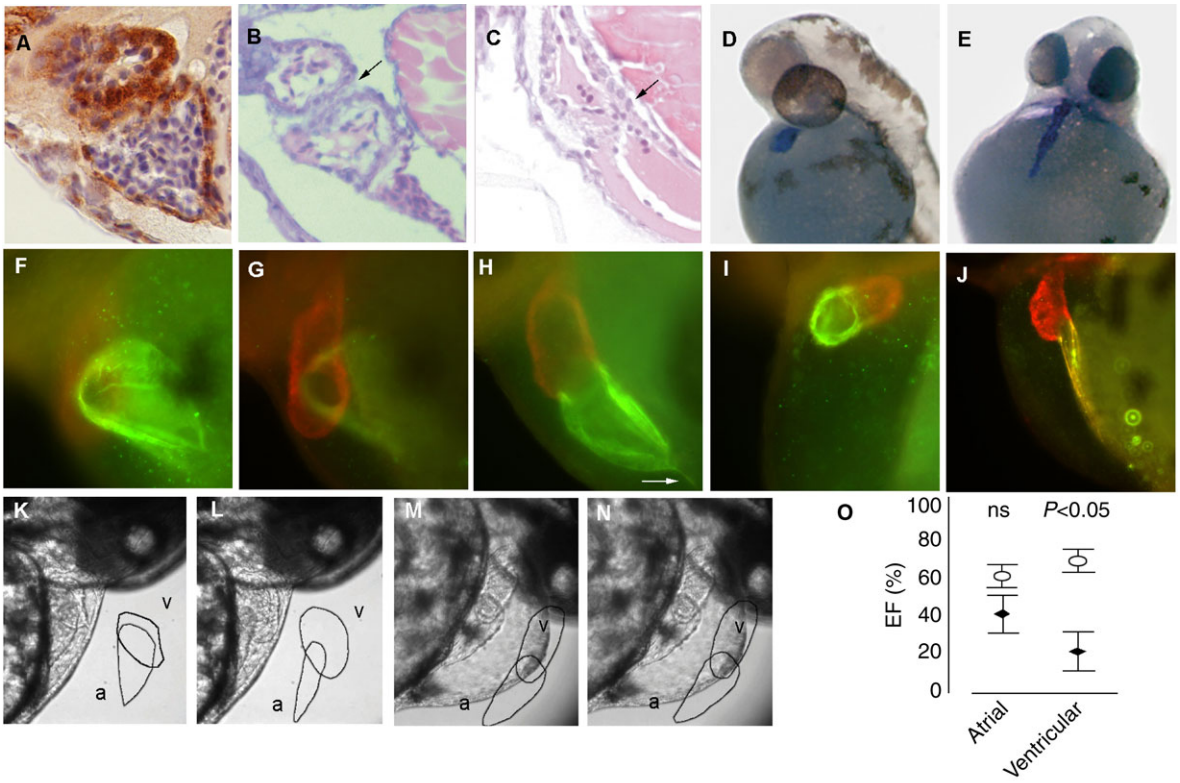


Fig. 5. Cardiac development and function in morphants. Fxr1 is abundant in normal hearts at 72 h.p.f. (hours postfertilisation) and is identified by Affi5 antibody in the thick walled ventricle and thinner walled atrium. At 48 h.p.f. the atrioventricular region is clearly seen in haematoxylin and eosin stained sections from control embryos (A). There is a waist at this level and cuboidal cells are forming the atrioventricular cushions (B, arrow). In morphants, the atrioventricular cushions are forming but the shape of the atrium and ventricles remain tubular and the atrioventricular waist is not prominent (C, arrow). By 56 h.p.f. whole mount *in situ* hybridisation for *cardiac myosin light chain 2* (*cmlc2*) demonstrates the normal looped globular heart in control embryos (D) but in 4 ng morphants the heart persists as a linear structure (E). Whole mount immunofluorescent labelling with MF20 and S46 antibodies. MF20 (red) identifies both atrial and ventricular myocytes whereas S46 (green) detects atrial specific myosin. Hence, ventricular myocytes appear red and atrial myocytes green/yellow. It is not possible to capture the atrium and ventricle of a 48 h.p.f. control morphant in the same focal plane. In (F) the atrium is in focus and the ventricle is not whereas in (G) the ventricle is in the focal plane whilst the atrium is not. In a 48 h.p.f. 4 ng morphant the heart has not looped, the atrium and ventricle remain in the same linear arrangement and in the same focal plane. There is a small amount of pericardial fluid (arrow) (H). In some embryos injected with 8 ng MO, the cells connecting the atrium to the sinus venosus had snapped by 48 h.p.f., such that the disconnected heart continued to beat within a large pericardial collection; no remnant of atrial tissue remained at the yolk sac surface (I). In some morphants the atrium became stretched but, by contrast, the ventricle maintained a compacted form (J). Sequential video microscopy images of a control morphant (K,L) and a 4 ng morphant (M,N) at 72 h.p.f. The atrial end–diastolic phase coincides with the end of ventricular systole (K,M) and similarly the end of atrial systole coincides with ventricular end diastole (L,N). In the morphant shown, there is almost no change in volume during atrial contraction (M,N) compared with the atrial contraction of the control embryo (K,L). Similarly there is minimal reduction in ventricular volume in the *fxr1* morphant seen as narrowing of the short axis (N,M), compared with the large reduction in ventricular volume in the WT embryo (L,K). The difference between percentage ejection fraction (EF%) in control and morphant embryos was statistically significant for ventricular function but not atrial contraction (O). a, atrial; v, ventricular.

very recently an opposite role for Fxr1 has been demonstrated. In response to serum starvation Fxr1 together with AGO2 acts as a translational activator (Vasudevan and Steitz, 2007).

Although the zebrafish only has a single atrium and ventricle, compared with the parallel chamber arrangement in mammals, it has been shown to be an excellent vertebrate model for heart development (Cripps and Olson, 2002). Importantly, although heart chambers appear to develop normally we have shown that looping does not occur and overall contractile function is poor in these morphants. Interestingly, it is clear that the primary heart tube forms normally in the partial absence of Fxr1. The accumulation of pericardial oedema is the first overt evidence that the heart may be failing to meet the demands of the developing embryo. Although the exact cause of this pericardial oedema is unknown, it is presumed to be comparable with the fluid accumulation seen, for example, in human patients with heart failure. Although a disturbance of osmoregulation in the embryo or abnormalities of renal function might cause a pericardial collection, the severe heart dysfunction measured in these morphants is of a magnitude to completely account for these effects, particularly in the presence of additional vascular abnormalities due to abnormal tail formation. Genetic causes for a failure of looping with normal chamber formation are uncommon, although recently Walton et al. reported that the repression motif of Friend of GATA 1 (*Fog1*), a multi-type zinc finger protein, is required for cardiac looping in zebrafish (Walton et al., 2006). Whilst it is possible that disruption of *Fog1* or a similar gene may produce a failure of looping in the *fxr1* morphants, looping is also an active process and generation of stress forces within the heart tube are required (Latacha et al., 2005). It is possible that failure of force transduction between cells of the heart tube might prevent looping. This is particularly appealing given that contractile function in the morphants was significantly diminished and some of the hearts snapped from their venous connections at the time of looping. It is possible that Fxr1 plays a

role in the transport of specific mRNAs to costameres within the cardiomyocytes as well as skeletal myocytes. However, although disturbed dystrophin localisation may be relevant in skeletal muscle, we have not been able to identify dystrophin in the developing zebrafish heart within the first seven days of development (B.C., unpublished observations) and zebrafish dystrophin mutants do not have an overt cardiac phenotype (Bassett and Currie, 2003). It is possible however that other proteins playing similar functional roles to dystrophin may be dependent on Fxr1 for trafficking.

Thus, Fxr1 deficiency might disturb the normal alteration of myocardial cell morphology, possibly due to actin polymerisation (Latacha et al., 2005) and therefore prevent looping forces being generated as well as the proper organisation of contractile actin–myosin arrays. Thus, there are several ways in which a lack of Fxr1 may produce cardiac structural failure and contractile weakness. Certainly, there is the possibility that early expression of fundamental heart transcription factors, such as Mef2c, Nkx2.5 and GATA factors may be disturbed as with the expression pattern of MyoD. It is also possible that interference with actin polymerisation could prevent looping and also creation of actin filaments within contractile arrays as discussed above. Finally, the construction of intercellular connections at the intercalated discs (adherens junctions and connexons) between cardiomyocytes may be abnormal, and this seems possible given the snapping heart phenotype. The investigation of these possibilities is the focus of ongoing investigation. Interestingly, two recent reports described an alteration of FXR1 expression in muscle disease, indicating a role of FXR1P in the pathophysiology of these specific disorders (Davidovic et al., 2008; Orengo et al., 2008).

In summary, we have demonstrated that *fxr1* plays a role of in the development of skeletal muscle both in the early specification of myotomes and in the localisation of dystrophin to the myoseptae. Furthermore, and importantly, we have demonstrated a failure of normal cardiac looping, severe cardiomyopathy and separation of the atrium from its venous connections. Given the severity of this cardiac phenotype, it is not surprising that the *Fxr1* mice die in the neonatal period, and no human correlates have been described (Mientjes et al., 2004). This zebrafish model of Fxr1 knockdown therefore provides an important model to analyse the *fxr* family function, which is not readily possible in other ways. Importantly *fxr1* is the main family member expressed in muscle and cardiac tissue and the effects of knockdown cannot be masked by redundancy of function of the other family members in nervous tissue.

The authors would like to thank Dr J. Bakkers, Hubrecht laboratory Utrecht for providing the *MyoD* and *Cmlc* probes. Photography and graphics by Ruud Koppenol and Tom de Vries Lentsch. This study was supported by a grant from ZonMW 908-02-010 (R.W.). We would like to thank Dr E. Khandjian for providing pT7TS/FXR1 iso7.

## REFERENCES

**Ashley, C., Jr, Wilkinson, K. D., Reines, D. and Warren, S. T.** (1993). FMR1 protein: conserved RNP family domains and selective RNA binding. *Science* **262**, 563-568.

**Bakker, C. E., Verheij, C., Willemsen, R., Vanderhelm, R., Oerlemans, F., Vermey, M., Bygrave, A., Hoogeveen, A. T., Oostra, B. A., Reyniers, E. et al.** (1994). Fmr1 knockout mice: a model to study fragile X mental retardation. *Cell* **78**, 23-33.

**Bakker, C. E., de Diego Otero, Y., Bontekoe, C., Raghoe, P., Luteijn, T., Hoogeveen, A. T., Oostra, B. A. and Willemsen, R.** (2000). Immunocytochemical and biochemical characterization of FMRP, FXR1P, and FXR2P in the mouse. *Exp. Cell Res.* **258**, 162-170.

**Bassett, D. I. and Currie, P. D.** (2003). The zebrafish as a model for muscular dystrophy and congenital myopathy. *Hum. Mol. Genet.* **12 Spec No 2**, R265-R270.

**Bechara, E., Davidovic, L., Melko, M., Bensaid, M., Tremblay, S., Grosgeorge, J., Khandjian, E. W., Lalli, E. and Bardoni, B.** (2007). Fragile X related protein 1 isoforms differentially modulate the affinity of fragile X mental retardation protein for G-quartet RNA structure. *Nucleic Acids Res.* **35**, 299-306.

**Bontekoe, C. J., McIlwain, K. L., Nieuwenhuizen, I. M., Yuva-Paylor, L. A., Nellis, A., Willemsen, R., Fang, Z., Kirkpatrick, L., Bakker, C. E., McAninch, R. et al.** (2002). Knockout mouse model for Fxr2: a model for mental retardation. *Hum. Mol. Genet.* **11**, 487-498.

**Cripps, R. M. and Olson, E. N.** (2002). Control of cardiac development by an evolutionarily conserved transcriptional network. *Dev. Biol.* **246**, 14-28.

**Davidovic, L., Sacconi, S., Bechara, E. G., Delplace, S., Allegra, M., Desnuelle, C. and Bardoni, B.** (2008). Alteration of expression of muscle specific isoforms of the fragile X related protein 1 (FXR1P) in facioscapulohumeral muscular dystrophy patients. *J. Med. Genet.* **45**, 679-685.

**Dube, M., Huot, M. E. and Khandjian, E. W.** (2000). Muscle specific Fragile X related protein 1 isoforms are sequestered in the nucleus of undifferentiated myoblast. *BMC Genet.* **1**, 1-4.

**Ekker, S. C. and Larson, J. D.** (2001). Morphant technology in model developmental systems. *Genesis* **30**, 89-93.

**Engels, B., Van't Padje, S., Blonden, L., Severijnen, L. A., Oostra, B. A. and Willemsen, R.** (2004). Characterization of Fxr1 in *Danio rerio*: a simple vertebrate model to study costamere development. *J. Exp. Biol.* **207**, 3329-3338.

**Feng, Y., Absher, D., Eberhart, D. E., Brown, V., Malter, H. E. and Warren, S. T.** (1997). FMRP associates with polyribosomes as an mRNP, and the I304N mutation of severe fragile X syndrome abolishes this association. *Mol. Cell* **1**, 109-118.

**Huot, M. E., Bisson, N., Davidovic, L., Mazroui, R., Labelle, Y., Moss, T. and Khandjian, E. W.** (2005). The RNA-binding protein fragile X-related 1 regulates somite formation in *Xenopus laevis*. *Mol. Biol. Cell* **16**, 4350-4361.

**Ingham, P. W. and Kim, H. R.** (2005). Hedgehog signalling and the specification of muscle cell identity in the zebrafish embryo. *Exp. Cell Res.* **306**, 336-342.

**Keegan, B. R., Meyer, D. and Yelon, D.** (2004). Organization of cardiac chamber progenitors in the zebrafish blastula. *Development* **131**, 3081-3091.

**Kimmel, C. B., Ballard, W. W., Kimmel, S. R., Ullmann, B. and Schilling, T. F.** (1995). Stages of embryonic development of the zebrafish. *Dev. Dyn.* **203**, 253-310.

**Latacha, K. S., Remond, M. C., Ramasubramanian, A., Chen, A. Y., Elson, E. L. and Taber, L. A.** (2005). Role of actin polymerization in bending of the early heart tube. *Dev. Dyn.* **233**, 1272-1286.

**Mientjes, E. J., Willemsen, R., Kirkpatrick, L. L., Nieuwenhuizen, I. M., Hoogeveen-Westerveld, M., Verweij, M., Reis, S., Bardoni, B., Hoogeveen, A. T., Oostra, B. A. et al.** (2004). Fxr1 knockout mice show a striated muscle phenotype: implications for Fxr1p function *in vivo*. *Hum. Mol. Genet.* **13**, 1291-1302.

**Orengo, J. P., Chambon, P., Metzger, D., Mosier, D. R., Snipes, G. J. and Cooper, T. A.** (2008). Expanded CTG repeats within the DMPK 3′ UTR causes severe skeletal muscle wasting in an inducible mouse model for myotonic dystrophy. *Proc. Natl. Acad. Sci. USA* **105**, 2646-2651.

**Samarel, A. M.** (2005). Costameres, focal adhesions, and cardiomyocyte mechanotransduction. *Am. J. Physiol. Heart Circ. Physiol.* **289**, H2291-H2301.

**Sandler, H. and Dodge, H. T.** (1968). The use of single plane angiocardiograms for the calculation of left ventricular volume in man. *Am. Heart J.* **75**, 325-334.

**Schwerte, T., Voigt, S. and Pelster, B.** (2005). Epigenetic variations in early cardiovascular performance and hematopoiesis can be explained by maternal and clutch effects in developing zebrafish (*Danio rerio*). *Comp. Biochem. Physiol. A Mol. Integr. Physiol.* **141**, 200-209.

**Siomi, H., Matunis, M. J., Michael, W. M. and Dreyfuss, G.** (1993). The pre-mRNA binding K protein contains a novel evolutionarily conserved motif. *Nucleic Acids Res.* **21**, 1193-1198.

**Tamanini, F., Meijer, N., Verheij, C., Willems, P. J., Galjaard, H., Oostra, B. A. and Hoogeveen, A. T.** (1996). FMRP is associated to the ribosomes *via* RNA. *Hum. Mol. Genet.* **5**, 809-813.

**Tapscott, S. J.** (2005). The circuitry of a master switch: myod and the regulation of skeletal muscle gene transcription. *Development* **132**, 2685-2695.

**Thisse, C., Thisse, B., Schilling, T. F. and Postlethwait, J. H.** (1993). Structure of the zebrafish snail1 gene and its expression in wild-type, spadetail and no tail mutant embryos. *Development* **119**, 1203-1215.

**Van't Padje, S., Engels, B., Blonden, L., Severijnen, L. A., Verheijen, F., Oostra, B. A. and Willemsen, R.** (2005). Characterisation of Fmrp in zebrafish: evolutionary dynamics of the fmr1 gene. *Dev. Genes Evol.* **215**, 198-206.

**Vasudevan, S. and Steitz, J. A.** (2007). AU-rich-element-mediated upregulation of translation by FXR1 and Argonaute 2. *Cell* **128**, 1105-1118.

**Walton, R. Z., Bruce, A. E., Olivey, H. E., Najib, K., Johnson, V., Earley, J. U., Ho, R. K. and Svensson, E. C.** (2006). Fog1 is required for cardiac looping in zebrafish. *Dev. Biol.* **289**, 482-493.

**Weinberg, E. S., Allende, M. L., Kelly, C. S., Abdelhamid, A., Murakami, T., Andermann, P., Doerre, O. G., Grunwald, D. J. and Riggleman, B.** (1996). Developmental regulation of zebrafish MyoD in wild-type, no tail and spadetail embryos. *Development* **122**, 271-280.

**Yelon, D., Horne, S. A. and Stainier, D. Y.** (1999). Restricted expression of cardiac myosin genes reveals regulated aspects of heart tube assembly in zebrafish. *Dev. Biol.* **214**, 23-37.